5.2 INTERACTION OF TURBULENT DEFLAGRATIONS WITH REPRESENTATIVE FLOW OBSTACLES

B. Durst, N. Ardey and F. Mayinger
Lehrstuhl A für Thermodynamik
Technische Universität München
D-80 290 München, Germany

Abstract

In the case of a gradual release of hydrogen in the course of an assumed, severe accident in a light water reactor, the combustion will normally start out as a slow deflagration. Acceleration of an initially slow flame due to interactions of chemical kinetics and turbulent heat and mass transfer can result in very high flame speeds. Therefore, in order to assess hydrogen mitigation techniques, detailed knowledge about flame acceleration and interaction of flames with obstacles is required. The reported investigations are aimed at the investigation of the mechanisms responsible for turbulent flame acceleration and improving present correlations for estimates and models for numerical simulations of hydrogen combustion processes. A medium-scale square cross-section setup is employed, using flow obstacles with shapes representative for reactor containments. The global flame speed is deduced from measurements using thermocouples, pressure transducers and photodiodes. Measurements using a two-component LDA-system are being carried through in order to correlate global flame spread and local turbulence parameters. Results indicate that low blockage-ratio obstacles only marginally influence the flame, as disturbances which are induced remain local to the vicinity of the obstacle and die out very quickly downstream thereof. Flow visualizations by means of a Schlieren setup indicate very complex flow structures in the vicinity of obstacles. The results are being used to validate turbulent reaction models. A model based on probability density functions (pdf) of assumed shape has been developed and initial calculations are presented.

Introduction

Combustion of hydrogen formed in the course of an assumed, severe loss-of-coolant accident is one of the main issues of safety considerations in connection with light water reactors. Igniting the hydrogen before concentrations sensitive to violent combustion modes (e.g. fast deflagrations or even detonations) are reached, is an appealing approach, as the resulting loads on the structure of the containment

remain low and it can be assumed that the hydrogen concentration is considerably decreased if not completely removed. However, open questions in connection with this approach still remain and it is necessary to regard aspects of the combustion which may leed to potential hazards. An area which must be considered in this respect is the influence of turbulence on combustion processes. If the ignition threshold is set sufficently low, the combustion will start out as a slow deflagration. However, it has been shown [1] that the interaction of chemical kinetics and heat and mass transfer due to turbulent mixing and momentum exchange processes can significantly accelerate flames to limits where damage of the containment structure must be expected.

Hydrogen explosions in confined geometries can be thought of as turbulent flamefronts superimposed on a highly turbulent expansion flow which itself is formed by the heat release due to the combustion and accoustic effects of generated and reflected pressure waves. The pressure increase caused by the flame front depends strongly on its propagation velocity. Immediately after the ignition of an H_2-air mixture, an unstable feed-back mechnism arises. A cellular flame structure develops and generates turbulence ahead of the flame which, by interaction with the flame front, yields turbulent acceleration. In a smooth channel this process can reach a steady state in which the flame front propagates steadily at a constant velocity below the mixture's limit for critical flame speeds with strong precursor shocks. Further flame acceleration is achieved by generation of additional turbulence in the expansion flow ahaed of the flame e.g. by interaction of the flow with obstacels and obstructions. It is, therefore, necessary to study the mechanisms which lead to this acceleration and to classify obstacles bound to repeatedly occur in reactor containments according to their influence.

The work carried through in the framework of the present project comprises experimental investigations in order to enhance the insight into the mechanisms of flame acceleretion and to obtain a database for validation purposes, as well as theoretical analysis in order to further develop numerical models capable of simulating turbulent combustion processes.

Experimental Investigations

The experiments presently being performed are carried through in a horizontal explosion tube with a square cross-section (268×268 mm) and a length of 3.5 m (cf. Fig. 1). Single flow obstacles can be exposed to the propagating flame front in a special tube segment which allows optical access and can be mounted at any position in the sequence of tube elements. The obstacles chosen are representative for typical shapes bound to exist in containments like pipes, pipe bundles, grids, door openings and different half size bodies (cf. Fig. 2).

The instrumentation used to determine global and local propagation information of the flame includes fast thermocouples which record the temperature rise caused

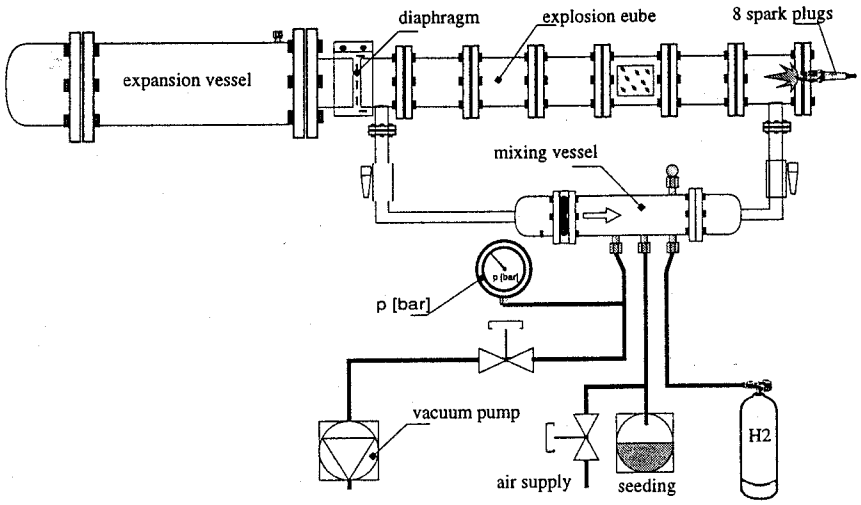

Figure 1. Experimental setup

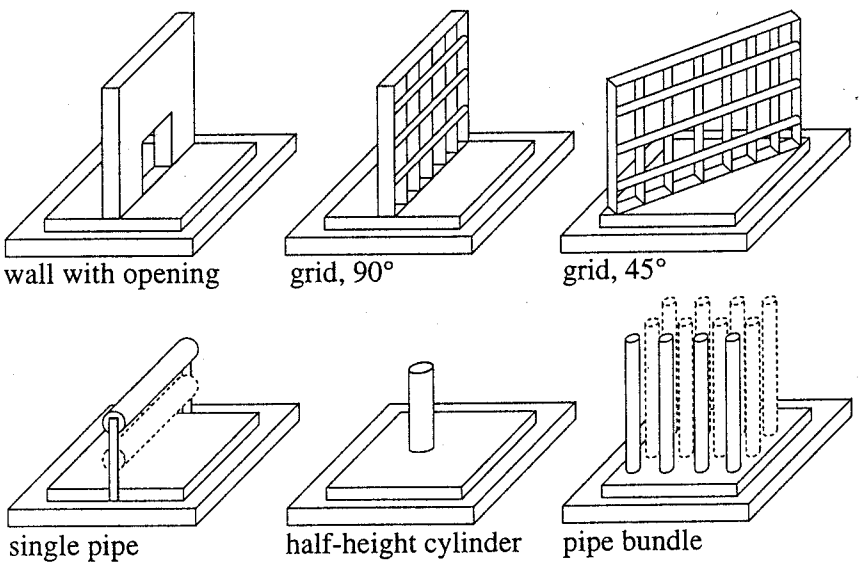

Figure 2. Obstacle configurations

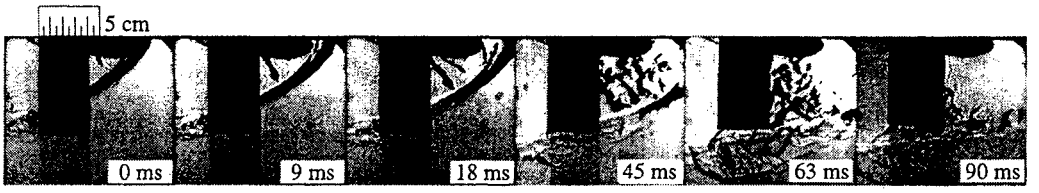

(a) **Vertical Half-Height Cylinder, 9 vol.% H_2**

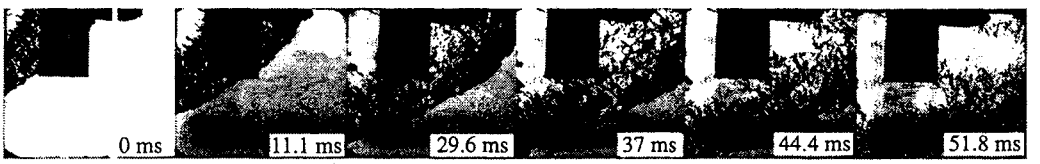

(b) **Vertical Half-Height Cylinder, 12 vol.% H_2**

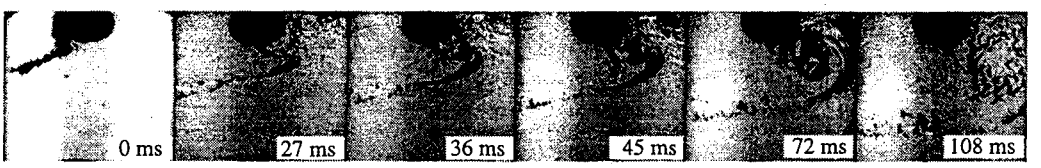

(c) **Horizontal Pipe, Upper Position, 9 vol.% H_2**

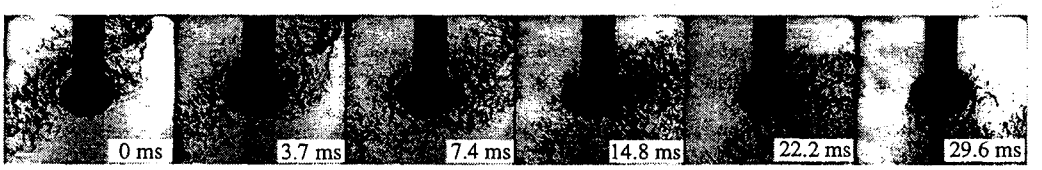

(d) **Horizontal Pipe, Center Position, 12 vol.% H_2**

Figure 3. Schlieren ciné records

by the passing flame, positioned at equal spacing along the top and bottom of the tube, in order to account for bouyancy effects. Photodiodes register the light emmitted by the flame and the pressure rise is recorded at two positiones along the tube and, in the case of the wall with an opening, on the obstacle's front and rear face. Local velocity components are determined using a two-component laser Doppler-setup (LDA). High-speed Schlieren cinematography is used to visualize the integral flame structure.

Fig. 3 shows a representative selection of Schlieren records of the flame propagation in the vicinity of a half-height cylinder inserted from the top of the

explosion tube (cf. Figs. 3(a),3(b)) and a horizontal pipe at different positions in the explosion tube (Figs. 3(c) andr3(d)). The flow structures that arise are very complex. The increase in turbulence with increase in H_2 concentration can readily be observed by comparison of eg. Figs. 3(a) and 3(b), showing the vertical half-height cylinder at two different H_2 concentrations. Due to the higher level of turbulence, the 12 vol.% flame does not seperate as early at the obstcale and the wake region behind the obstacle is smaller. At 12 vol.%, the flame covers the whole cross section of the explosion tube. The part of the flame that is affected by the obstacle, therefore, is smaller than for the 9 vol.%-flame. In spite of these significant differences, the thermocouple and photo-diode records do not show any difference to the experiments without obstacle.

In the case of the horizontal pipe at the upper position and the 9 vol.%-flame, a phenomenon which is particularly interesting could be visualized. Due to the acceleration of the flow between the obstacle and the upper explosion tube wall,

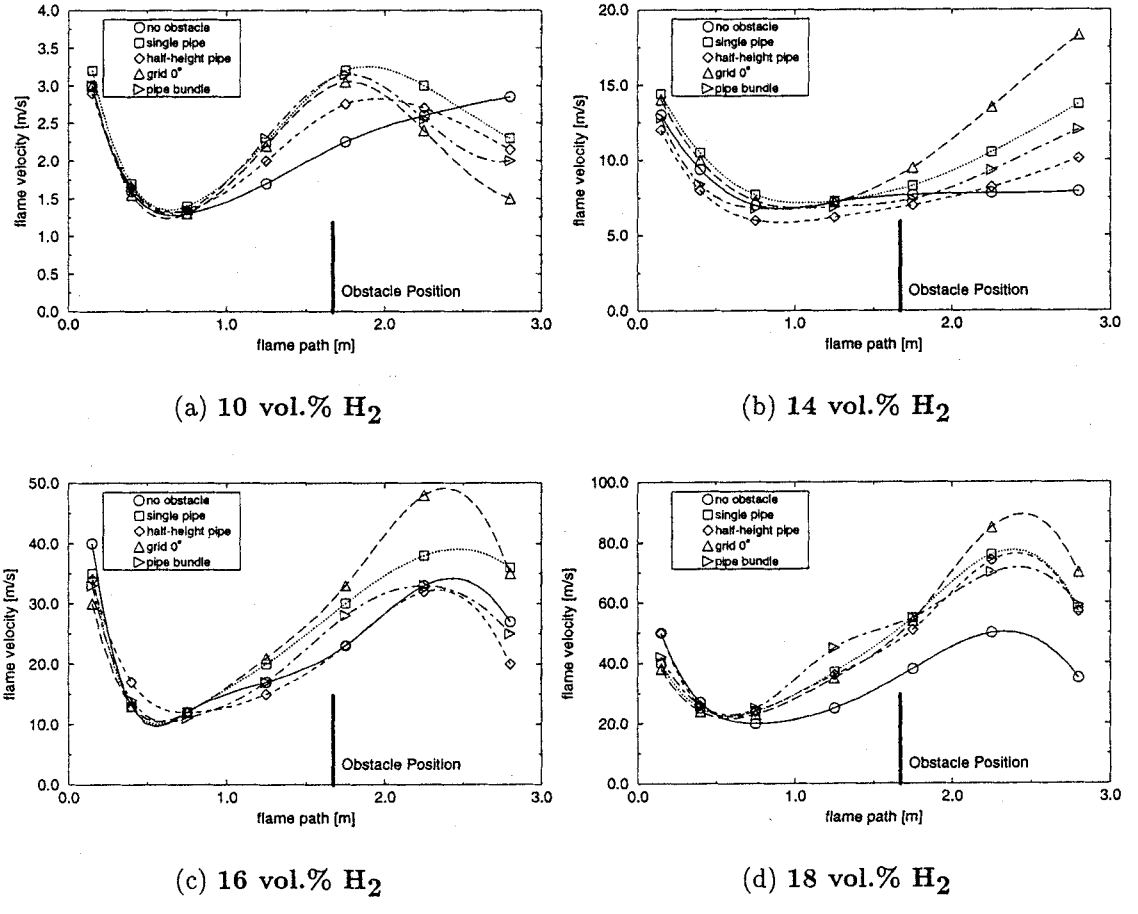

(a) **10 vol.% H_2**

(b) **14 vol.% H_2**

(c) **16 vol.% H_2**

(d) **18 vol.% H_2**

Figure 4. Flame velocity vs. flame path for obstacles with low blockage ratios

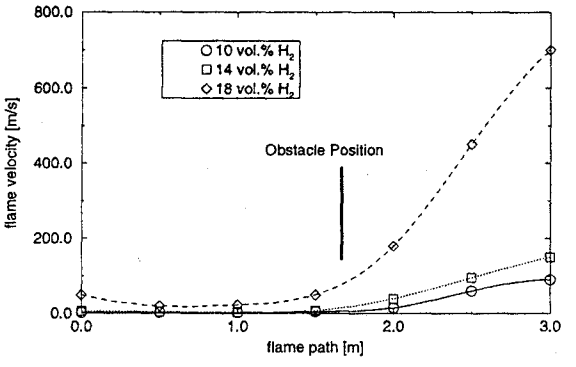

Figure 5. Flame velocity vs. flame path for high blockage ratio obstacle

and interaction with pressure waves, the flame is pushed back at the lower part of the obstacle. Away from the obstacle, the flame burns unobstructed and consequently rolls up to form a large-scale vortex cylinder which is stabilized in the wake of the obstacle. Apparently, it is constantly fed by unburned gas which is entrained along the outer surface of the vortex. In this case the thermocouple measurements along the top of the explosion tube show a slight acceleration of the flame which reaches twice the speed it had at the beginning of the tube (cf. Fig. 4). This situation is quite the same for the case of a 12 vol.%-flame with the pipe positioned at the center of the explosion tube. The part of the flame which influences the upper row of thermocouples therefore seems to be decoupled from the stagnating vortex.

The respective thermocouple records are shown in Fig. 4. It is found that low blockage ratio obstacles at the investigated positions in the explosion tube do not severely accelerate the flame front to violent combustion modes. The maximum flame speed found at 18 vol.% H_2 with the grid at 0° inclination does not exceed 90 m/s.

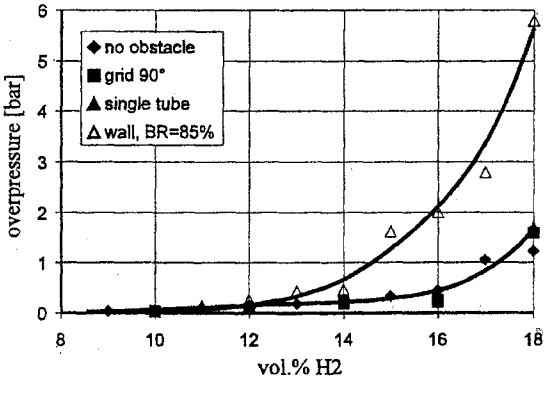

Figure 6. Maximum overpressures for different obstacles

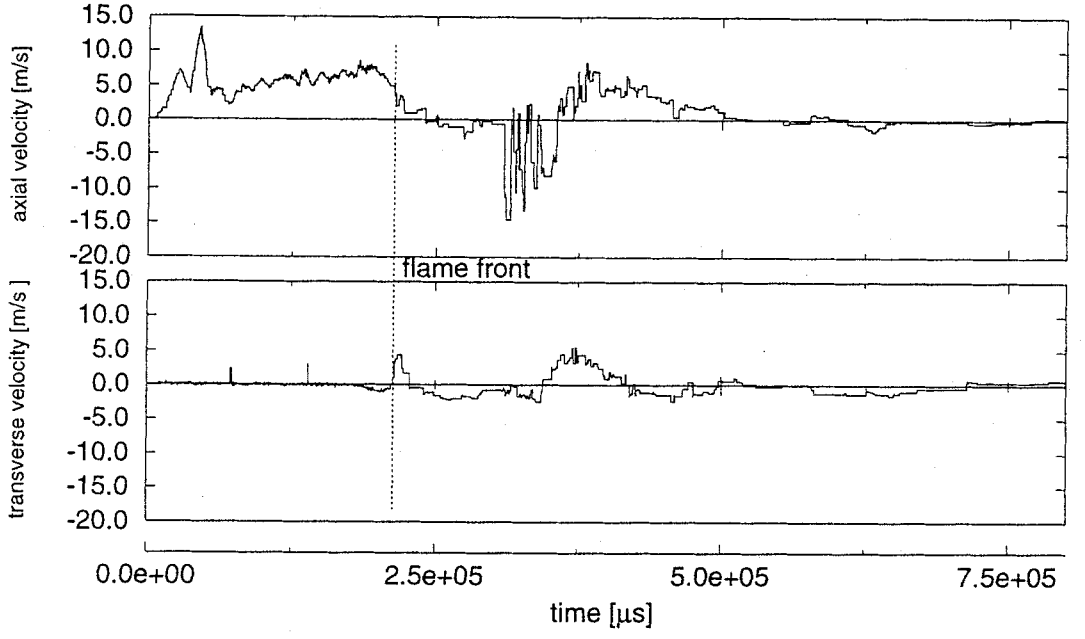

(a) 14 vol.% H_2 – no obstacle

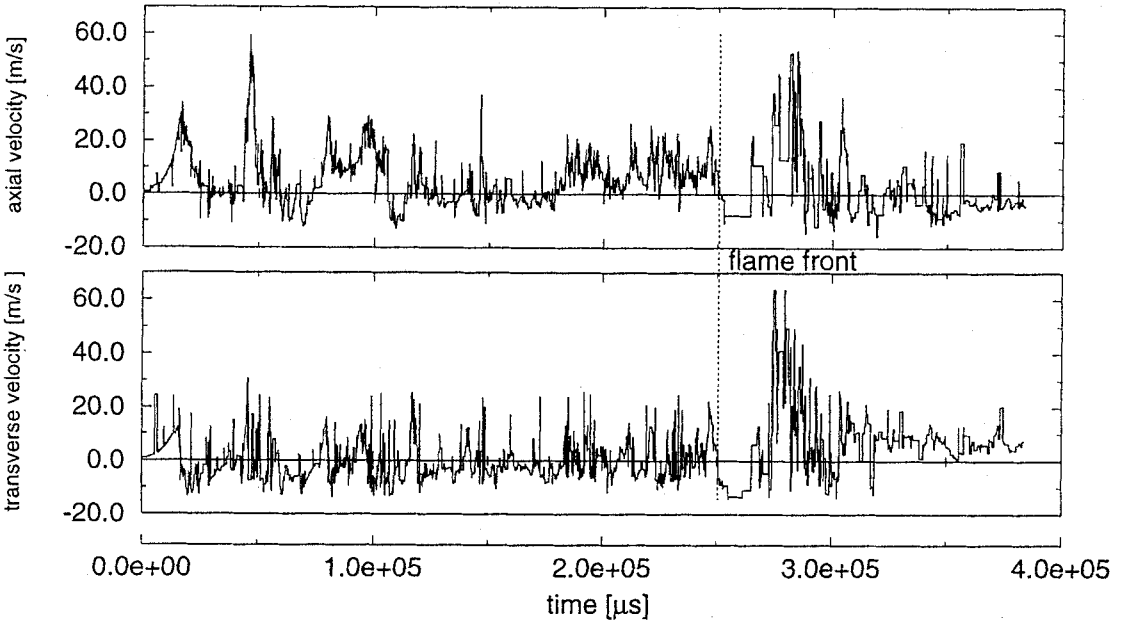

(b) 14 vol.% H_2 – wall obstacle

Figure 7. Local velocity samplings using LDA

This situation is completely different for the wall obstacle with a high blockage ratio (85%). In this case, the flow is forced to seperate and form a jet behind the obstacle. Flame speeds reached range up to 700 m/s, as shown in Fig. 5, causing maximum overpressures of 6 bar in the tube (cf. Fig. 6). It should be noticed that the generated pressure rises strongly depend on the geometry confining the flame, and that the peak pressure are specific for the applied test setup. Maximum flame speeds appear to be a more consisitent criterion for a ranking of obstacles. Comparisons with investigations carried through at BATTELLE GmbH [2] indicate agreement in this respect.

The intense effect of the high blockage ratio wall obstacle can also be seen in the LDA-records. The intense turbulence level is indicated by strong fluctuations of the signal in comparison to the situation without any obstacle (cf. Fig. 7). The velocities also increase strongly. The ratio of turbulent velocity fluctuations to laminar burning speed increases from $\frac{u'}{s_L} \approx 2$ to $\frac{u'}{s_L} \approx 40$.

Numerical Modelling

The aim of enhancing presently existing combustion models is to reach a point where the model is capable of realistically predicting turbulent deflagration processes. It is the fact that the deflagrations under consideration involve highly turbulent expansion flows which, besides the well-known models for the turbulent closure problem, necessitates models also for the chemical reaction rate.

The set of equations which governs a compressible flow problem involving chemical reactions comprises balance equations for mass conservation (continuity):

$$\frac{\partial \rho}{\partial t} + \frac{\partial}{\partial x_i}(\rho u_i) = 0,$$

conservation of species mass fractions (for $r = 1, \ldots N-1$ species):

$$\frac{\partial(\rho Y_r)}{\partial t} + \frac{\partial}{\partial x_i}(\rho u_i Y_r) = \frac{\partial}{\partial x_i}\left(\Gamma_r \frac{\partial Y_r}{\partial x_i}\right) + R_r,$$

momentum conservation:

$$\frac{\partial(\rho u_j)}{\partial t} + \frac{\partial}{\partial x_i}(\rho u_i u_j) = -\frac{\partial p}{\partial x_j} + \frac{\partial \tau_{ij}}{\partial x_i} + S_{uj},$$

and energy conservation:

$$\frac{\partial(\rho H)}{\partial t} - \frac{\partial P}{\partial t} + \frac{\partial}{\partial x_i}(\rho u_i H) = -\frac{\partial q_i}{\partial x_i} + \frac{\partial u_j \tau_{ij}}{\partial x_i} + S_H,$$

together with equations of state. We consider an ideal gas as a Newtonian fluid, for which:

$$\frac{p}{\rho} = M R_u T,$$

and:

$$\tau_{ij} = \mu\left(\frac{\partial u_i}{\partial x_j} + \frac{\partial u_j}{\partial x_i}\right) + \frac{2}{3}\mu\frac{\partial u_k}{\partial x_k}\delta_{ij}.$$

The total enthalpy H is defined as $H = h + \frac{1}{2}u_i^2$ with h as the the static enthalpy from $h = \sum_{r=1}^{N} Y_r h_r$. The molecular energy transport q_i in direction i is taken as $q_i = -\lambda\frac{\partial T}{\partial x_i} - \sum_{r=1}^{N}\Gamma_r h_r \frac{\partial Y_r}{\partial x_i}$ and the molecular weight of the mixture is given by $M = \sum_{r=1}^{N} n_r M_r$.

When using direct numerical simulation (DNS) all length scales of turbulence need to be resolved, and it can be shown that the number N_G of gridpoints required to resolve a three-dimensional geometry is:

$$N_G \sim \left(\frac{Re}{10}\right)^{9/4}.$$

For engineering problems the Reynold's number Re is of the order of 10^3 – $10^6, 10^7$ or even greater. Taking into account that for flows involving chemical reactions the timescales are even smaller, it is evident that DNS presently cannot be regarded as a feasible tool for engineering calculations.

For the above reason, we resort to time-averaging the balance eqution according to Reynolds. Instantaneous variables are split into mean and fluctuating part (cf. Fig. 8):

$$\phi = \bar{\phi} + \phi' \quad \text{with} \quad \bar{\phi} = \lim_{T\to\infty}\frac{1}{T}\int_{t_0}^{t_0+T}\phi\, dt,$$

or rather, as we are dealing with variable density flows, density weighted time-averaging:

$$\bar{\rho}\tilde{\phi} = \lim_{T\to\infty}\frac{1}{T}\int_{t_0}^{t_0+T}\rho\phi\, dt = \overline{\rho\phi} \quad \text{so that} \quad \phi = \tilde{\phi} + \phi''.$$

The averaged balance equations then read:

$$\frac{\partial\bar{\rho}}{\partial t} + \frac{\partial}{\partial x_i}(\bar{\rho}\tilde{u}_i) = 0,$$

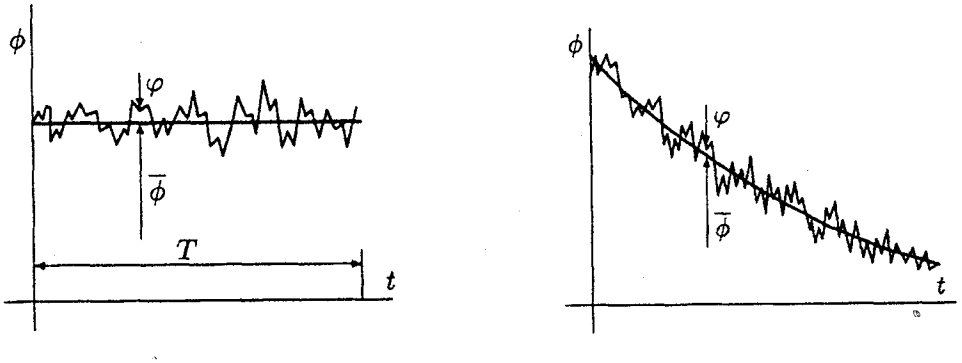

Figure 8. Time-averaging procedure for steady and transient flows

$$\frac{\partial \bar{\rho}\tilde{Y}_r}{\partial t} + \frac{\partial}{\partial x_i}(\bar{\rho}\tilde{u}_i\tilde{Y}_r) = \frac{\partial}{\partial x_i}\left(\Gamma_r \frac{\partial \tilde{Y}_r}{\partial x_i} - \overline{\rho u_i'' Y_r''}\right) + \bar{R}_r; \quad r = 1, \ldots N-1, \qquad (1)$$

$$\frac{\partial(\bar{\rho}\tilde{u}_j)}{\partial t} + \frac{\partial}{\partial x_i}(\bar{\rho}\tilde{u}_i\tilde{u}_j) = -\frac{\partial \bar{p}}{\partial x_j} + \frac{\partial}{\partial x_i}(\bar{\tau}_{ij} - \overline{\rho u_j'' u_i''}) + \bar{S}_{uj},$$

$$\frac{\partial(\bar{\rho}\tilde{H})}{\partial t} - \frac{\partial \bar{P}}{\partial t} + \frac{\partial}{\partial x_i}(\bar{\rho}\tilde{u}_i\tilde{H}) =$$
$$- \frac{\partial}{\partial x_i}(\bar{q}_i + \overline{\rho u_j'' h''}) + \frac{\partial}{\partial x_i}\left(\tilde{u}_j(\bar{\tau}_{ij} - \overline{\rho u_j'' u_i''}) + \overline{u_j'' \tau_{ij}''}\right) + \bar{S}_H.$$

The closure problems arise from the cross-correlation terms $\overline{\rho u_j'' u_i''}$, $\overline{\rho u_j'' h''}$ and $\overline{u_j'' \tau_{ij}''}$ which are not related to mean values and, therefore, represent additional unknowns for the set of equations. As a turbulence model to close the set of equations with respect to these terms, we use the well-known k–ε model with enhancements to consider compressibility.

The present contribution, however, will not focus on the details of turbulence modelling, but rather on the closure problem related to the chemical source term $\bar{R}_r$ in (1). We regard a global one-step irreversable reaction of fuel and oxidizer to products:

$$\text{Fuel} + s\text{Oxidizer} \rightarrow \text{Products}.$$

The instantaneous reaction rate for the fuel species of this reaction can be written in terms of fluctuating quantities as:

$$R_{fu} = M_{fu}\left(\frac{\rho Y_{fu}}{M_{fu}}\right)\left(\frac{\rho Y_{ox}}{M_{ox}}\right)^s A_1 e^{-E_1/RT}. \qquad (2)$$

However, as this equation is highly nonlinear, its mean value $\bar{R}_{fu}$ which is required in Eq. (1) for the fuel species cannot be estimated simply by introducing mean values into this equation:

$$\bar{R}_{fu} \neq M_{fu}\left(\frac{\bar{\rho}\bar{Y}_{fu}}{M_{fu}}\right)\left(\frac{\bar{\rho}\bar{Y}_{ox}}{M_{ox}}\right)^s A_1 e^{-E_1/R\tilde{T}},$$

but rather from

$$\bar{R}_{fu} = M_{fu}\left(\frac{\bar{\rho}\bar{Y}_{fu}}{M_{fu}}\right)\left(\frac{\bar{\rho}\bar{Y}_{ox}}{M_{ox}}\right)^s A_1 e^{-E_1/R\tilde{T}}(1+F),$$

where F represents a polynomial of cross-correlations of T'', Y_{fu}'' and Y_{ox}''. Failing to consider this term can lead to errors up to three orders of magnitude [3]. The number of correlations involved, prohibits trying to model every single term. It is therefore necessary to model the chemical reaction rate as a whole. Approaches to this problem include semi-empirical combustion models such as the Eddy-Breakup model of Spalding [4] or the Eddy-Dissipation-Concept of Magnussen and

Hjertager [5], flamelet approaches [6] and more recently models employing probability density functions (pdf) [7]. The latter can be distinguished into two groups, one which solves transport equations for the pdf and the other which precribes a shape of the pdf. For the present work we use pdfs of assumed shape.

The probability density $P(\phi)$ is defined such that $P(\phi)d\phi$ is the probability that ϕ lies in a small range $d\phi$ around a particular function $\phi(x_i, t)$. If ϕ depends on various variables $\rho, T, Y_N, \ldots$, the mean value of ϕ can then be calculated as:

$$\bar{\phi}(x_i, t) = \int_\rho \int_T \int_{Y_n} R_n(\rho, T, Y_N, \ldots)\tilde{P}(\rho, T, Y_N, \ldots; x_i, t)d\rho\, dT\, dY_n \ldots$$

In the above equaton, $P(\rho, T, Y_N, \ldots; x_i, t)$ denotes the joint pdf depending on $\rho, T, Y_N, \ldots$. In our case we reduce the dependency by defining:

$$\rho = f_1(Y_p), \quad T = f_2(Y_p), \quad Y_{fu} = f_3(Y_p) \quad \text{and} \quad Y_{ox} = f_4(Y_p). \tag{3}$$

and a variable c that specifies the reaction progress:

$$c = \frac{Y_p}{Y_{p,\infty}}. \tag{4}$$

Using Eqs. (3) and (4), Eq. (2) can be simplified so that the reaction rate is merely a function of c:

$$R_n(\rho, T, Y_N, \ldots) \rightarrow R_n(c).$$

As c is defined only for $0 \leq c \leq 1$, the mean reaction rate can then be calculated from:

$$\bar{R}_n = \int_0^1 R_n(c)P(c; x_i, t)dc.$$

As already mentioned, the shape of $P(c; x_i, t)$ is assumed in the present work. It has been shown [3] that the results of pdf calculations are relatively insensitive to the precise shape used. As a natural approach, we use a Gaussian distribution with the parts extending outside the range of c clipped into Dirac functions at the bounds, as shown in Fig. 9.

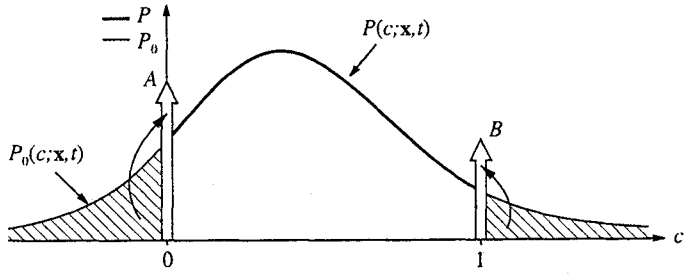

Figure 9. Clipped Gaussian distribution

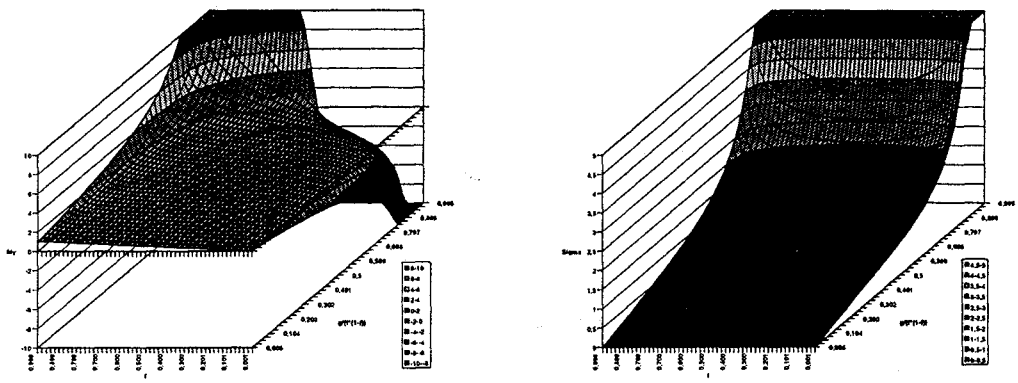

Figure 10. Tables for μ and σ

This functions is defined as:

$$P(c;x_i,t) = P_0(c;x_i,t)\,[H(c) - H(c-1)] + A(x_i,t)\delta(c) + B(x_i,t)\delta(1-c),$$

with:

$$P_0(c;x_i,t) = \frac{1}{\sigma\sqrt{2\pi}} \exp\left[-\frac{1}{2}\left(\frac{c-\mu}{\sigma}\right)^2\right],$$

where μ and σ denote the mean and variance of the distribution, respectively. These two parameters can be determined from $\tilde{c}$ and $\tilde{c}''^2$, as a scale for the mean of the fluctions of c, for which additional balance equations are solved. The clipped Gaussian distribution has the drawback that, given $\tilde{c}$ and $\tilde{c}''^2$, it cannot explicitly be solved for μ and σ. Some root-finding algorithm must be employed, which for the number of gridpoints involved, requires substantial computational time. For

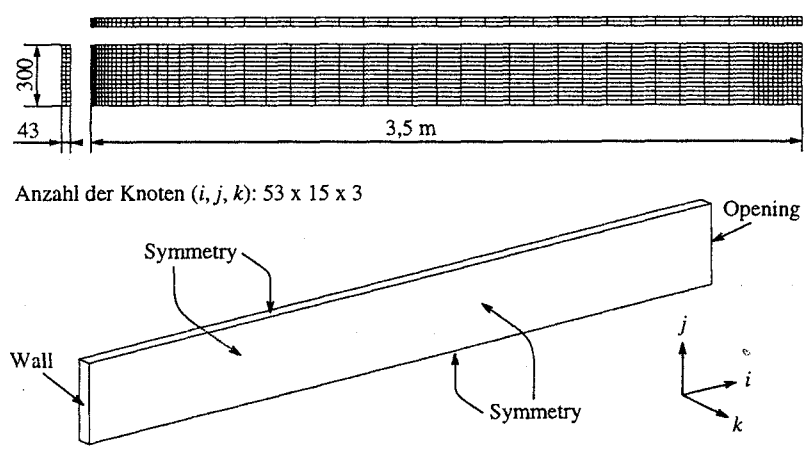

Figure 11. Computational grid and boundary conditions

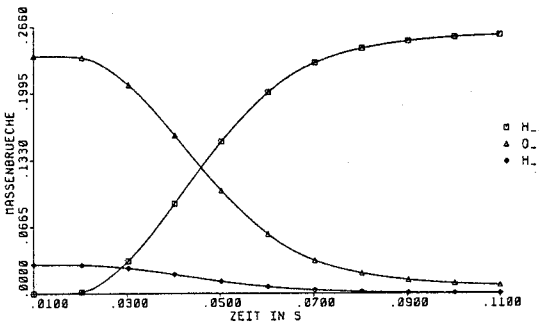

(a) massfractions at $x = 0.1$ m vs. time

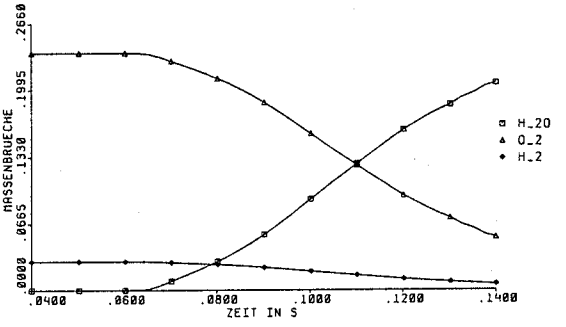

(b) massfractions at $x = 1.5$ m vs. time

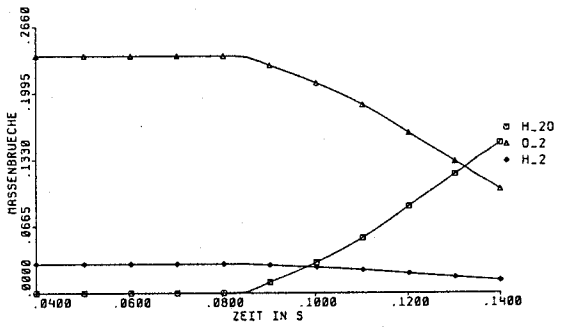

(c) massfractions at $x = 3.3$ m vs. time

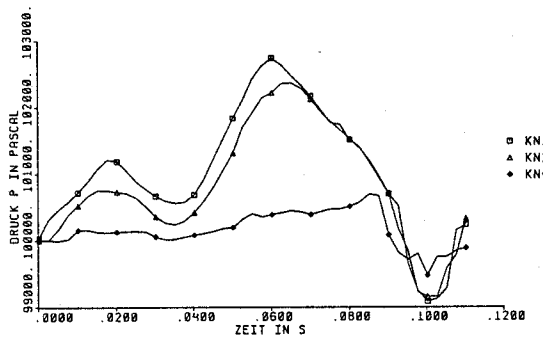

(d) pressures at the 3 locations vs. time

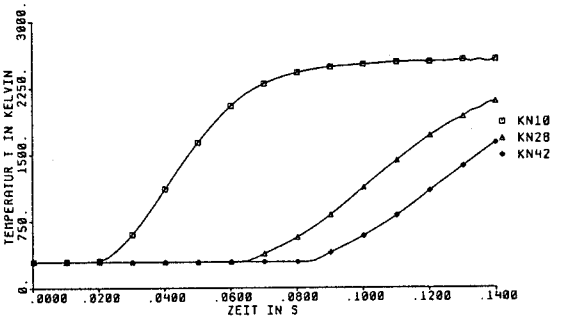

(e) temperatures at the 3 locations vs. time

Figure 12. Results of calculations

this reason, these two values are tabulated following [8], as shown in Fig. 10. The required values can then be interpolated during the calculation from the tables.

The computational domain that is used for the initial calculations is shown in Fig. 11. We use $53 \times 15 \times 3$ points in the x, y and z-direction. The pdf-model was implemented into a commercial CFD-code using user-definable routines. Fig. 12 shows results of the calculations. The calculations are in agreement with the experimental findings for the case without any obstacle. Main characteristics of the combustion process such as the double pressure rise or the timescale of the rise in temperatures are predicted well.

Concluding Remarks

The experimental investigations carried through in the course of the present project have shown that for low blockage ratio obstacles in the square cross-section tube, the influence of the obstacles remains very limited. Additional turbulence is generated mainly in the vicinity of the obstacle and dies out very quickly downstream of the obstacle. High blockage ratio obstacles such as a simulated wall with an opening or walking grids inclined to the flow, however, lead to accelerations of the flame. From comparison with measurements carried through in smaller-scale setups, it was found, that the maximum flame speed is a more consistent criterion for ranking obstacles according to their influence on the flame than the peak pressure, as the latter depends strongly on the geometry of the confinement rather than on the obstacle. In the further course of the project visualizations of the reaction zone using laser induced (predissociation) flourescence will be carried through, in order to be able to analyse the interaction of turbulence and chemical reaction precisely.

A closure model for the chemical reaction rate based on probability density functions of assumed shape has been developed and implemented into a commercial CFD-code. The shape assumed for the pdf is that of a clipped Gaussian distribution. A reaction progress variable is used so that a single variable pdf can be employed. Calculation of the Gaussian distributian is speeded up by precalculating the dependencies and using a table look-up procedure during the calculation. The results of initial calculations show agreement with experimental findings. The model will be extended to multidimensional pdfs, in order to allow for more complex chemical reaction mechanisms.

Acknowledgements

It is gratefully acknowledged that the work presented in this paper has been supported by the German Ministry of Education, Science, Research and Technology.

Nomenclature

A_1 reaction rate constant
c reaction progress variable
E_1 reaction rate constant
H total enthalpy, Heaviside function
h static enthalpy
M molar weight
n number of moles
N number species
q_i molecular energy transport in ith direction
s burning velocity
t time
r reaction rate
R gas constant
s stoichiometric coefficient
S additional source terms in balance equations
T Temperature
u_i instantaneous velocity in ith direction
u_i' velocity fluctuation in ith direction
x_i ith coordinate direction
Y mass fraction

Greek Symbols

Γ effective molecular diffusion coefficient
δ_{ij} unit tensor
δ Dirac-peakfunction
μ dynamic viscosity
ρ density
ϕ representative scalar
τ_{ij} viscous stress tensor

Subscripts

fu fuel
L laminar
ox oxidizer
r rth chemical species
u universal
∞ completely burned state

References

[1] R. Beauvais, F. Mayinger, and G. Strube. Turbulent flame acceleration–mechanisms and significance for safety considerations. *Int. J. Hydrogen Energy*, 19(8):701–708, 1994.

[2] J. Tenschert and T. Kanzleiter. Wasserstoff-Deflagrations-Experimente in einer kleinmaßstäblichen Versuchsanlage DN400. Technischer Fachbericht BF-R68.145-302, BATELLE Ingenieurtechnik GmbH, 1995.

[3] W. P. Jones and J. H. Whitelaw. Calculation methods for reacting turbulent flows: A review. *Combust. and Flame*, 48:1–26, 1982.

[4] D. B. Spalding. Mixing and chemical reaction in steady confined turbulent flames. In *13th (int.) Symposium on Combust.*, pages 643–657. The Combustion Institute, 1971.

[5] B. F. Magnussen and B. H. Hjertager. On mathematical modelling of turbulent combustion with special emphasis on soot formation and combustion. *16th (int.) Symposium on Combust.*, pages 719–729, 1976.

[6] N. Peters. Laminar flamelet concepts in turbulent combustion. In *21st (int.) Symposium on Combust.*, pages 1231–1250. The Combustion Institute, 1986.

[7] S. B. Pope. Pdf methods for turbulent reacting flows. *Prog. in Energy and Combust. Sci.*, 11:119–192, 1985.

[8] F. C. Lockwood and A. S. Naguib. The prediction of the fluctuations in the properties of free, round-jet, turbulent diffusion flames. *Combust. and Flame*, 24:109–124, 1975.

[9] N. Ardey, F. Mayinger, and B. Durst. Influence of transport phenomena on the structure of lean, premixed hydrogen flames. In *Transactions vol. 73.* American Nuclear Society, 1995.